

Current-Phase Relation and Josephson Inductance of Superconducting Cooper Pair Transistor

A. Paila,^{1,*} D. Gunnarsson,¹ J. Sarkar,¹ M. A. Sillanpää,¹ and P. J. Hakonen¹

¹*Low Temperature Laboratory, Helsinki University of Technology, Espoo, Finland*

We have investigated the Josephson inductance L_J of a Superconducting Cooper Pair Transistor (SCPT). We traced the inductance using microwave reflection measurements on a tuned resonance circuit in which a SCPT was mounted in parallel to a ~ 200 pH strip line inductance. When the inverse of the Josephson inductance, determined on the charge-phase bias plane for a SCPT with a Josephson to Coulomb energy ratio of $E_J/E_C = 1.75$, is integrated over the phase, we obtain a current-phase relation, which is strongly non-sinusoidal near the charge degeneracy point.

PACS numbers: 85.25.Cp, 85.35.Gv, 74.78.Na, 74.25.Fy

Josephson effect is one of the most spectacular phenomena in quantum coherent matter. In addition to superconductors, it has been studied in superfluids^{1,2} and Bose-Einstein condensates^{3,4}. The coupling between the ordered states across a Josephson tunnel junction can be described by the < Josephson energy $E(\varphi)$ where φ denotes the phase difference between the order parameter fields on the opposite sides of the junction. Equivalently, the nature of a Josephson junction can be characterized by its current-phase relation (CPR) $I(\varphi) = \frac{2\pi}{\Phi_0} \frac{dE}{d\varphi}$ where $\Phi_0 = \frac{h}{2e}$ is the flux quantum. In a regular tunnel barrier junction, the CPR is sinusoidal, which leads to a non-linear dynamical inductance of $L_J^{-1} = \frac{dI}{d\Phi} = \frac{2\pi}{\Phi_0} I_c \cos \varphi$ where $\Phi = \Phi_0 \varphi / 2\pi$ is the flux corresponding to the phase φ ⁵. In junctions with sinusoidal CPR, $|L_J|$ is π -periodic and the inductance changes sign at $\varphi = \pi/2$ and at $\varphi = 3\pi/2$. As the inverse inductance describes the energy exchange rate of the junction with its surrounding electrical circuit, we observe that the junction varies periodically between a circuit element either receiving or releasing energy, in a sinusoidal fashion in this case. In different kinds of junctions, for example, in superconducting quantum point contacts (QPC) and in diffusive SNS junctions, the CPR can be strongly non-sinusoidal⁶. In the outmost case, like in a QPC with near perfect transmission ($\tau \rightarrow 1$), $I(\varphi)$ becomes discontinuous^{7,8} and the region of negative Josephson inductance shrinks to zero. Similar discontinuous behavior takes place also in two symmetric, classical junctions in series⁹.

In a mesoscopic double junction device, charge quantization on the island between the junctions starts to play a role. This leads to phase fluctuations across the individual junctions, even if the total phase bias acts like a classical variable and can be fixed. As a consequence, the CPR is strongly modified from the classical result. The energy bands, calculable from the Schrödinger equation with the Coulombic term acting as the kinetic energy operator in the phase picture^{9,10}, are well known and these eigenenergies form the cornerstone of charge qubits as well as charge-phase qubits^{11,12,13}. A lot of energy spectroscopy has been performed on these energy levels which, however, does not probe the current-phase relation of the ground state unless assumptions on the

symmetry properties of the bands are made. Here we report measurements on the Josephson inductance of a superconducting Cooper pair transistor and determine its CPR. We present, for the first time to our knowledge, results on the current-phase relation that demonstrate the strongly non-sinusoidal character near the charge degeneracy point. Our results are based on accurate reflection measurements of a charge-phase qubit coupled to a microwave resonator.

In the superconducting state, a tunnel junction stores energy in the form of Josephson coupling energy according to $E = -E_J \cos(\varphi)$, where the Josephson energy E_J is related to the junction critical current I_C through $I_C = 2eE_J/\hbar$. According to electromagnetism, the inductance is defined by the differential of the total energy

$$L = \left(\frac{\partial^2 \mathcal{H}}{\partial \Phi^2} \right)^{-1} = \left(\frac{\Phi_0}{2\pi} \right)^2 \left(\frac{\partial^2 \mathcal{H}}{\partial \varphi^2} \right)^{-1}. \quad (1)$$

In the regime of small fluctuations, $\varphi \ll 1$, Eq. (1) yields for a single classical Josephson junction (JJ) a parametric inductance $L_J^0 = \hbar/(2eI_C^0)$. For arbitrary phase bias, one gets $L_J^{-1} = [L_J^0]^{-1} \cos \varphi$.

Although typically applied to single JJs, these concepts can be applied to general junction combinations like a single Cooper-pair transistor (SCPT) which consists of two JJs and one capacitively coupled gate electrode. The full description of SCPT's energy storing capabilities is governed by its Hamiltonian¹⁰

$$\hat{H} = E_C(\hat{n} - n_g)^2 - 2E_J \cos \frac{\varphi}{2} \cos \hat{\theta} + 2dE_J \sin \frac{\varphi}{2} \sin \hat{\theta}, \quad (2)$$

where $E_C = e^2/(2C)$ is the charging energy of the island, \hat{n} denotes the number of extra electron charges on the island, and $n_g = C_g V_g/e$ is gate-voltage-induced charge in units of single electron on the gate with capacitance C_g . \hat{n} is conjugate to $\hat{\theta}/2$, where $\hat{\theta}$ is the superconducting phase on the island. The asymmetry of the two Josephson junctions of the SCPT is described by $d = (E_{J1} - E_{J2})/2E_J$. As we are interested in the phase response, the electrostatic energy associated with the gate capacitance may be neglected here, contrary to the case in Ref. 14 where Josephson capacitance was

considered. In order to get the Josephson inductance, the eigenenergies of Hamiltonian of Eq. (2) have to be solved first^{15,16}.

Qualitative analysis can be performed in the charge basis taking only two charge states into account. Then, the Hamiltonian can be written in terms of Pauli spin matrices as¹³

$$\hat{H} = -\frac{1}{2} (B_x \hat{\sigma}_x + B_y \hat{\sigma}_y + B_z \hat{\sigma}_z), \quad (3)$$

where the magnetic field components are $B_z = 4E_C(1 - n_g)$, $B_x = 2E_J \cos(\varphi/2)$ and $B_y = 2dE_J \cos(\varphi/2)$. By differentiating the energy eigenvalues, one obtains an analytic form for the inductance of the ground state

$$\frac{L_{J\downarrow}}{(\Phi_0/2\pi)^2} = \frac{\frac{8\sqrt{2}}{E_J} \left(1 + \frac{8}{\gamma^2} (1 - n_g)^2 + \cos \varphi\right)^{3/2}}{\left(4 + \frac{32}{\gamma^2} (1 - n_g)^2\right) \cos \varphi + 3 + \cos 2\varphi}, \quad (4)$$

where γ denotes the ratio $\gamma = E_J/E_C$. Because of the symmetry in the two level approximation one gets $L_{J\uparrow} = -L_{J\downarrow}$ for the excited state. When $\gamma \ll 1$, the two level approximation describes the energy bands accurately but, when $\gamma \sim 1$, more charge states are needed. $L_{J\downarrow}$ calculated from the two level approximation, compared to the measured data in Fig. 4 below, is found to fall short and numerical calculations including more levels are needed to make a detailed comparison. Nevertheless, Eq. (4) reveals clearly the main features: 1) the supercurrent is strongly suppressed with lowering γ , and 2) the non-harmonic character grows when approaching the charge degeneracy point¹⁶.

In the experiment, the SCPT's reactive response was measured in the L-SET (inductively read single-electron transistor) configuration¹⁷, where the junctions are embedded in an electric LC-oscillator circuit (see also Refs. 18,19,20). The L-SET sample was fabricated using a standard e-beam lithography process followed by evaporation of aluminum films at two different angles of incidence. Circuit diagram of the L-SET sample is shown in Fig. 1. The SCPT is attached in parallel with an inductor that is realized using an on-chip microstrip loop. The length of the loop is $300 \mu\text{m}$, which yields $L_m = 168 \text{ pH}$ inductance. The two parallel capacitors of the resonator are made by patterning two large plates ($1.3\text{mm} \times 1.3\text{mm}$) on the substrate (see Fig. 2 of Ref. 21). The bottom plate of the capacitor is formed by a 150 nm thick niobium ground plane layer under the Si_3N_4 dielectric layer whose thickness is around 300 nm . The measured resonance frequency yields for the capacitors $C = 396 \text{ pF}$, which agrees well with the parallel plate result using $\epsilon_r = 7.5$ for Si_3N_4 . Because our capacitors are non-ideal, we have to take into account their ac-losses by introducing a shunting resistance whose value $R = 1.4 \text{ k}\Omega$ was determined from the Q -factor of the resonator. The coupling capacitor $C_c = 6.5 \text{ pF}$, that decouples the oscillator from the driving coaxial cable, is a separate surface mount capacitor that is bonded with aluminum wires to

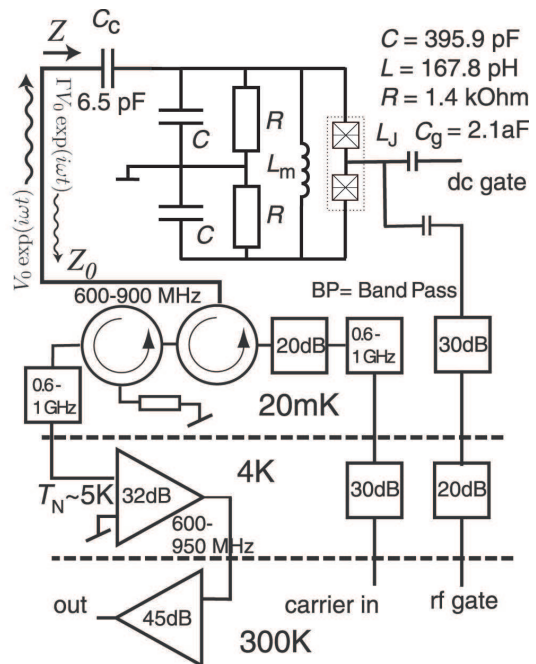


FIG. 1: The circuit diagram of our symmetrized L-SET device. Here the SCPT's Josephson inductance L_J is in parallel with an on-chip microstrip inductor L_m which form together the inductor in the LC-oscillator: $1/L = 1/L_J + 1/L_m$. C_c is the coupling capacitor that decouples the resonator from the driving signal generator.

the top pad of one of the capacitors. The gate modulation was $2e$ periodic and from the period we deduce $C_g = 2.1 \text{ aF}$. From the rf-spectroscopy we conclude that $E_c/k_B = 0.8 \text{ K}$, $E_J/k_B \approx 1.6 \text{ K}$, and the asymmetry parameter $d \approx 0.06$.

The Josephson inductance was measured using a microwave reflection measurement setup working around $f_m = 870 \text{ MHz}$. Continuous microwave signal was sent from one port of a vector network analyzer through a series of attenuators and a circulator to the sample. Part of the sent signal was reflected back to the transmission line due to the impedance mismatch between $Z_0 = 50 \Omega$ and the impedance of the resonator circuit, Z (see Fig. 1): $V_{out} = \Gamma V_{in}$, where $\Gamma = (Z - Z_0)/(Z + Z_0)$. The reflected signal was then taken from the third port of the circulator (isolation 18 dB), amplified with an array of cold and room temperature amplifiers and connected to the second channel of the network analyzer. The network analyzer gave us the magnitude signal and the phase argument (See Figs. 6 and 7 in Appendix I.) of the reflection coefficient which were used to calculate the effective impedance of the oscillator circuit. Using standard circuit analysis with linear elements, the Josephson

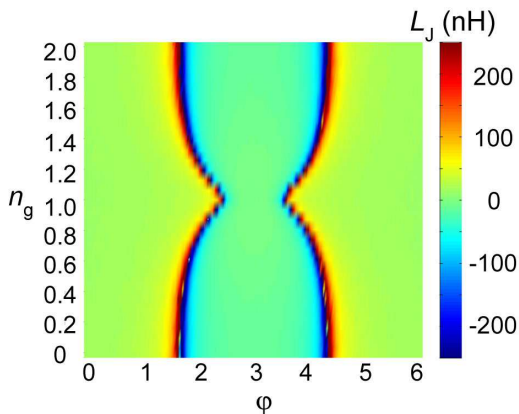


FIG. 2: Measured inductance of the ground state on the phase bias vs. gate charge plane (inductance scale limited to ± 250 nH). The plot was obtained using Eq. 5 and the data scans presented in the supplementary material.

inductance then can be calculated from the expression

$$L_J = \frac{1}{i\omega} \left[\left(\left(\left(\frac{1}{Z - Z_C} - \frac{1}{Z_R} \right)^{-1} - Z_R \right)^{-1} - \frac{1}{Z_L} \right)^{-1} \right], \quad (5)$$

where shorthand notations have been assigned to impedances of the circuit components $Z_C = (i\omega C_c)^{-1}$, $Z_L = i\omega L$, and $Z_R = (1/R + i\omega C)^{-1}$. The Josephson inductance, obtained by using the experimentally determined Z , is shown in Fig. 2. Ideally, the zero phase of the reflection signal should be determined separately for each bias point by plotting $\Gamma(f)$ parametrically on the Smith chart and looking for the symmetry axis of the resulting circle (see, e.g. Ref. 22). We, however, did this check only at one bias point and relied that the reference phase will not change substantially. The reflection magnitude scale was fixed using reflected signal far away from the resonance and the known circuit elements. The finite measurement signal averages the energy bands over phase direction. The power used in measurement, -129 dBm, corresponds to phase amplitude of 0.24 rad (p-p) and causes a 3 percent error to the inductance.

The corresponding inductance plot obtained from theory is shown in Fig. 3; five discrete charge states were used in the determination of the eigenvalues of Eq. (2). The general agreement between Figs. 2 and 3 is remarkable, except near the charge degeneracy point. At $n_g = 1$, the gap between the ground and excited states becomes small, about $\Delta/h = 3.8$ GHz, and the upper state can either be thermally excited at our effective noise temperature of ~ 40 mK, governed by the thermalization of our circulators, or by multiphoton processes due to the microwave drive at 872 MHz. In this case, the effective inductance is a mixture of the curvatures of the two energy levels making the analysis difficult. The mixing can, however, be used to determine the energy level occupation in systems where SCPT is considered as a qubit²³.

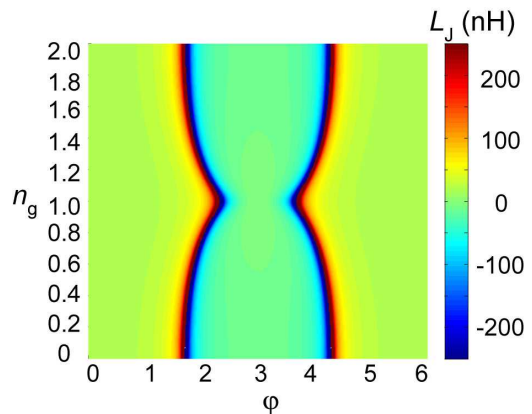


FIG. 3: Theoretically calculated L_J of the ground state on the φ vs. n_g plane ($|L_J| < \pm 250$ nH). The eigenvalues of the SCPT were numerically calculated using 5 charge states.

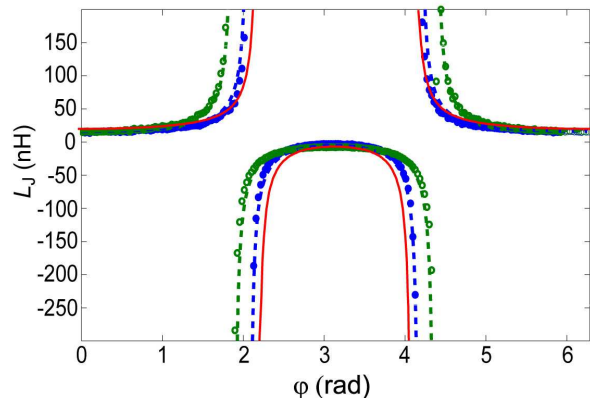


FIG. 4: Comparison of the measured Josephson inductance and the theoretical curves at two charge bias values 1.25e (filled/blue) and 1.51e (open/green). The red solid line illustrates L_J obtained from the two level approximation.

A more quantitative comparison between the experimental data and the theoretical prediction for $L_J(\varphi)$ is shown in Fig. 4. The theory models well the experimental result when $E_J/k_B = 1.5$ K is employed. The SCPT behaves as a non-linear inductor whose inductance is tunable by phase bias from a few nH to infinity (in ideal case). There exist substantial regions in the charge-phase plane where the Josephson inductance takes negative values, and the negative-value regime is diminished as the charge degeneracy point is approached.

The current-phase relation can be obtained by integrating the inverse of Josephson inductance: The relation $L_J^{-1} = \frac{\partial I}{\partial \Phi}$ yields $I(\varphi) = \frac{\Phi_0}{2\pi} \int_0^\varphi L_J^{-1} d\varphi + g(V_g)$ where the integration constant $g(V_g)$ must be set so that the zero level of $I(\varphi)$ is correct. The CPRs at gate charge values of $n_g = 0$ and $1e$ are displayed in Fig. 5. We observe that far away from the charge degeneracy point, $n_g \sim 0$, the CPR is nearly sinusoidal, while close to $n_g = 1$ the CPR becomes strongly non-sinusoidal. The measured behavior at $n_g = 0$ agrees quite well with theoretical curves calcu-

lated using $E_J/k_B = 1.5$ K. The measured variation of $I(\varphi)$ with gate charge is found to be 10% stronger than what the theory predicts. We believe this is partially due to the uncertainty in the parameter values obtained for E_J and E_C using energy level spectroscopy and, moreover, to the inaccuracy in the base level of $1/L_J$, which leads to an accumulation of error in the integration process.

Excitation of the SCPT from the ground state E_0 to the first excited level E_1 is another possible cause for the discrepancy between measured and calculated CPRs. We note that if the contribution of the upper level is included in simple terms (*i.e.* linear population-weighted addition of $1/L_J$ -values of the ground and excited states), then the correction would even worsen the agreement between theory and experiment. This is because the contribution of the level E_1 is smaller than that of the ground state, leading to reduced $1/L$ and its integral. Furthermore, inclusion of even higher bands yields similar conclusions as their values for $1/L_J$ are also small.

Effective energy bands with stronger curvature can be obtained if one assumes that the total energy is of the form $\mathcal{H}_S(\varphi) = p_0(\varphi)E_0(\varphi) + p_1(\varphi)E_1(\varphi)$ and that the populations $p_0(\varphi)$ and $p_1(\varphi)$ depend on φ on the time scale of $1/f_m$. Then the derivatives of $p_0(\varphi)$ and $p_1(\varphi)$ may make substantial modifications in the inductance and, thereby, in the integrated CPR. For a simple description, we assume a thermal distribution at effective system temperature T that governs the population of the upper state in the driven system according to

$$p_1(n_g, \varphi) = 1 - p_0(n_g, \varphi) = \left(1 + e^{\frac{\Delta}{k_b T}}\right)^{-1} \quad (6)$$

where $\Delta(n_g, \varphi) = E_1(n_g, \varphi) - E_0(n_g, \varphi)$. Below we will restrict ourselves only to a qualitative analysis by assuming that T can be regarded as a constant fitting parameter over the region of interest, *i.e.* for the data measured at $n_g = 1$.

Using this model, we get for the modified CPR $I_S(\varphi) = \frac{2\pi}{\Phi_0} \frac{d\mathcal{H}_S}{d\varphi}$ (bias parameter $n_g = 1e$ dropped)

$$I_S(\varphi) = I^0(\varphi) + \frac{\partial \Delta(\varphi)}{\partial \varphi} \left((1 - p_0) - \frac{\Delta}{k_b T} p_0^2 e^{-\frac{\Delta}{k_b T}} \right) \quad (7)$$

where $I^0(\varphi)$ is the CPR for the ground state. We have fitted Eq. (7) to our data in Fig. 5 at $n_g = 1e$ and find an improved agreement when taking $T = 0.28$ K; at $\varphi = \pi$ this corresponds to $p_1 = 0.30^{25}$. This value for T is quite high, well above the cross-over temperature of $1e - 2e$ periodicity in the gate modulation of our SCPT. Consequently, the bath temperature ought to be modified strongly by LZ transitions caused by the measurement drive. Far away from charge degeneracy, LZ-transitions are not effective and no modification of the CPR is needed in our comparison.

Non-sinusoidal CPRs have been reported in a number of Josephson junctions⁶. However, in superconducting Cooper pair transistors, where Coulomb energy plays an

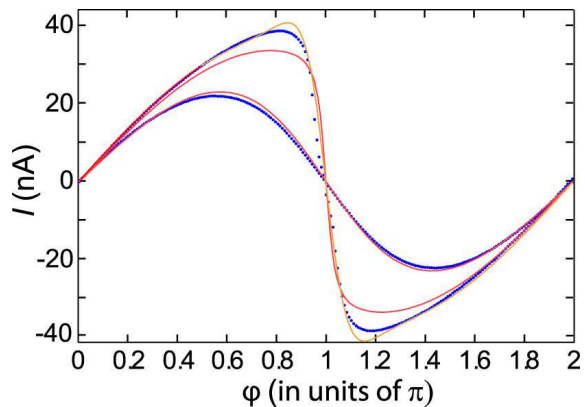


FIG. 5: Current-phase relations (CPR) obtained by integration of the inverse Josephson inductance at two gate charge values: 0 (nearly sinusoidal) and $1e$ (strongly non-sinusoidal). Experimental curves are denoted by blue dots while the red solid curves display the CPRs calculated from Eq. (2); the orange solid curve depicts the result calculated from Eq. (7) using $T = 0.28$ K.

important role, the results on (derivatives of) CPRs have remained few and unpersuasive^{24,26,27}. Closest to our work is the L_J measurement of Ref. 27 but their result was distinctly affected by a mixing of the ground and excited states due to nonequilibrium quasiparticles. Quasiparticles were also a problem in the determination of the ground state properties of Nb SCPTs in Ref. 24, where $1e$ periodicity in V_g was observed contrary to our clean $2e$ -periodic modulation. Moreover, Born and coworkers have employed Josephson inductance to characterize qubits²⁶, but their ratio of $E_J/E_C \sim 30\dots2$ was too high to make observations similar to ours.

Finally, we believe that our method for constructing the CPR will be useful also in studies of other exotic Josephson junctions where the critical current is small, like S-carbon nanotube-S junctions²⁸. Typically, critical currents in small junctions have been measured by applying current bias and recording switching current distributions²⁹. Even though it is not easy to accomplish, it has been recently shown that switching currents can be employed to measure current-phase relations in break junction samples under circumstances where a large Josephson junction is patterned in parallel with the break junction³⁰. Because there is no need for an extra junction, we think that our scheme is better suited for investigations of novel, fragile junctions where extra lithographic steps may be problematic.

In conclusion, using the phase and magnitude of reflected microwave signals, we have experimentally measured the Josephson inductance in a mesoscopic, superconducting double-tunnel-junction device, *i.e.*, we have determined the quantity that is dual to the Josephson capacitance^{14,31}. We have shown by integrating this Josephson inductance that the current-phase relation of a SCPT is strongly non-sinusoidal near its charge degeneracy point and that substantial tuning by the gate voltage

towards nearly sinusoidal CPR at $n_g \sim 0$ can be reached.

We thank Erkki Thuneberg, Alexander Zorin, Jani Tuorila, Tero Heikkilä, Matti Laakso and Mikko Paalonen for fruitful discussions and useful comments. This work was supported by the Academy of Finland and by the EU contract FP6-IST-021285-2.

I. APPENDIX

Scans containing the raw data employed in the analysis:

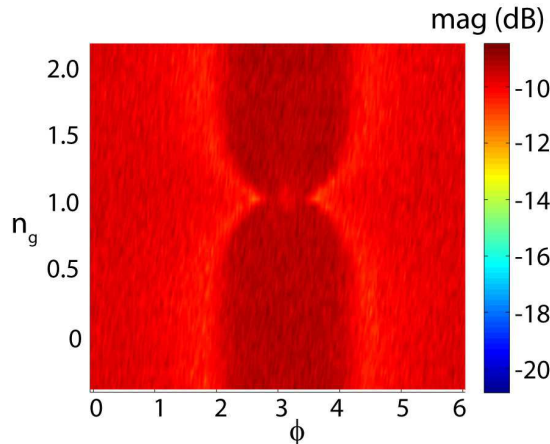


FIG. 6: Magnitude of the reflected signal as a function of the phase and charge bias on the superconducting Cooper pair transistor. The color scale in dB is given on the right; the full reflection corresponds to 9.8 dB.

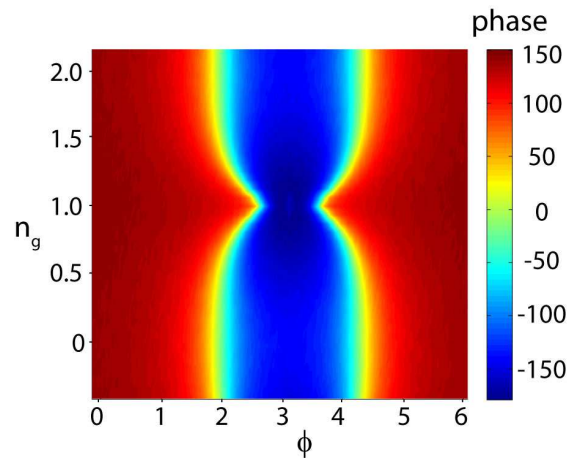


FIG. 7: Phase of the reflected signal in degrees as a function of the phase and charge bias. A correction of 25 degrees was made to the reference point of the reflection phase in order to symmetrize the $\Gamma(f)$ on the Smith chart.

* Corresponding author.

Electronic address: pjh@boojum.hut.fi

- ¹ O. Avenel and E. Varoquaux, Phys. Rev. Lett. **60**, 416 (1988).
- ² J. C. Davis and R. E. Packard, Rev. Mod. Phys. **74**, 741 (2002).
- ³ B. Anderson and M. Kasevich, Science **282**, 1686 (1998).
- ⁴ F. S. Cataliotti, S. Burger, C. Fort, P. Maddaloni, F. Minardi, A. Trombettoni, A. Smerzi, M. Inguscio, Science **293**, 843 (2001).
- ⁵ K. Likharev, *Dynamics of Josephson Junctions and Circuits* (Gordon Breach, Amsterdam, 1986).
- ⁶ A. A. Golubov, M. Y. Kupriyanov, and E. Il'ichev, Rev. Mod. Phys. **76**, 411 (2004).
- ⁷ I. O. Kulik and A. N. Omel'yanchuk, Sov. J. Low Temp. Phys. **3**, 459 (1977).
- ⁸ C. W. J. Beenakker and H. van Houten, Phys. Rev. Lett. **66**, 3056 (1991).
- ⁹ See e.g. K. A. Matveev, M. Gisselält, L. Glazman, M. Jonson, and R. Shekhter, Phys. Rev. Lett. **70**, 2940 (1993) or A. Zorin, Phys. Rev. Lett. **76**, 4408 (1996).
- ¹⁰ D. Averin and K. Likharev, *Mesoscopic Phenomena in Solids* (North Holland, New York, 1991).
- ¹¹ Y. Nakamura, Yu. Pashkin, and J. S. Tsai, Nature **398**,

786 (1999).

- ¹² D. Vion, A. Aassime, A. Cottet, P. Joyez, H. Pothier, C. Urbina, D. Esteve, and M. Devoret, Science **296**, 886 (2002).
- ¹³ Yu. Makhlin, G. Schön, and A. Shnirman, Rev. Mod. Phys. **73**, 357 (2001).
- ¹⁴ M. A. Sillanpää, T. Lehtinen, A. Paila, Yu. Makhlin, L. Roschier, and P. Hakonen, Phys. Rev. Lett. **95**, 206806 (2005).
- ¹⁵ A. Zorin, IEEE Trans. on Instr. and Meas. **46**, 299 (1997).
- ¹⁶ A. B. Zorin, Phys. C: Supercond. **368**, 284 (2002).
- ¹⁷ M. A. Sillanpää, L. Roschier, and P. Hakonen, Phys. Rev. Lett. **93**, 066805 (2004).
- ¹⁸ E. Il'ichev, V. Zakosarenko, L. Fritzsche, R. Stolz, H. E. Hoenig, H.-G. Meyer, M. Götz, A. B. Zorin, V. V. Khanin, A. B. Pavolotsky, and J. Niemeyer, et al., Rev. Sci. Instrum. **72**, 1882 (2001).
- ¹⁹ O. Naaman and J. Aumentado, Phys. Rev. B **73**, 172504 (2006).
- ²⁰ Shevchenko, S. N., Eur. Phys. J. B **61**, 187 (2008).
- ²¹ D. Gunnarsson, J. Tuorila, A. Paila, J. Sarkar, E. Thuneberg, Yu. Makhlin, and P. Hakonen, Phys. Rev. Lett. **101**, 256806 (2008).
- ²² D. Kajfez, *Q Factor* (Vector Forum, Oxford, 1994).

- ²³ M. Sillanpää, T. Lehtinen, A. Paila, Yu. Makhlin, and P. Hakonen, Phys. Rev. Lett. **96**, 187002 (2006).
- ²⁴ H. Zangerle, J. Könemann, B. Mackrodt, R. Dolata, S. V. Lotkhov, S. A. Bogoslovsky, M. Götz, and A. B. Zorin, Phys. Rev. B **73**, 224527 (2006).
- ²⁵ The worst case estimate for the Landau-Zener probability is $p_{LZ} \sim 0.05$ at the bias point $(n_g, \varphi) = (1, \pi)$; this is sufficient to produce a population of $p_1 = 0.30$ on the excited band when phase coherent addition of the tunneling amplitudes is accounted for. However, no Landau-Zener interference phenomena are observed in our data.
- ²⁶ D. Born, D. Shnyrkov, D. Krech, D. Wagner, D. Il'ichev, D. Grajcar, D. Hübner, and D. Meyer, Phys. Rev. B **70**, 180501 (2004).
- ²⁷ J. Könemann, H. Zangerle, J. Mackrodt, J. Dolata, and J. Zorin, Phys. Rev. B **76**, 134507 (2007).
- ²⁸ T. Tsuneta, L. Lechner, and P. J. Hakonen, Phys. Rev. Lett. **98**, 087002 (2007).
- ²⁹ See e.g. P. Joyez, P. Lafarge, A. Filipe, D. Esteve, and M. Devoret, Phys. Rev. Lett. **72**, 2458 (1994).
- ³⁰ M. L. D. Rocca, M. Chauvin, B. Huard, H. Pothier, D. Esteve, and C. Urbina, Phys. Rev. Lett. **99**, 127005 (2007).
- ³¹ T. Duty, G. Johansson, K. Bladh, D. Gunnarsson, C. Wilson, and P. Delsing, Phys. Rev. Lett. **95**, 206807 (2005).